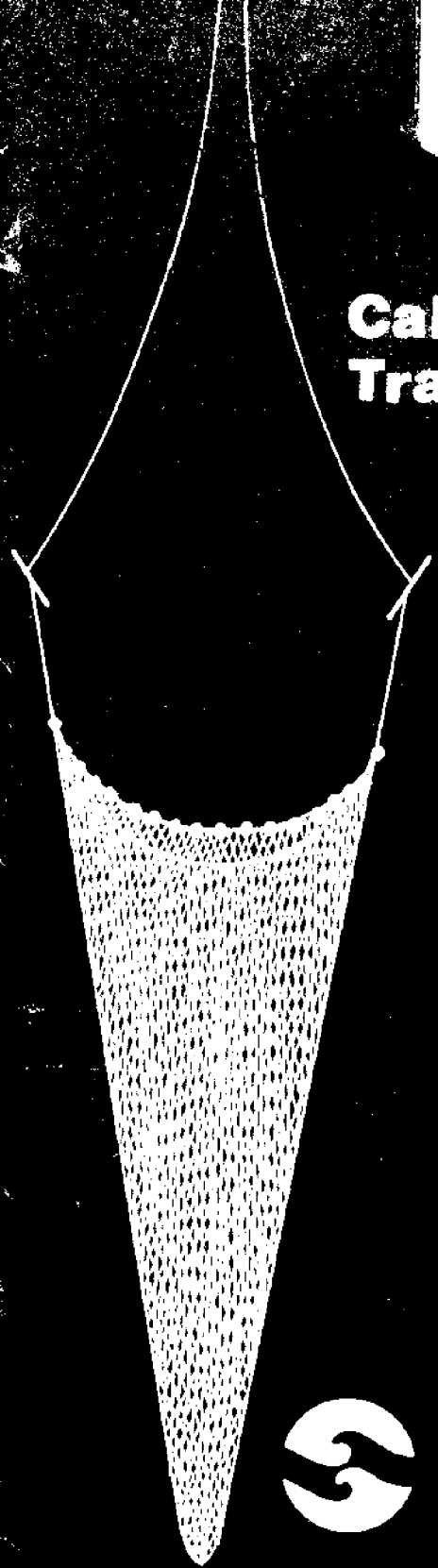

Calculation of Trawling Gear Drag

T. Kowalski
J. Giannotti

Ocean Engineering
Sea Grant

University of Rhode Island
Marine Technical Report No. 16

CALCULATION OF TRAWLING GEAR DRAG

T. Kowalski

J. Giannotti

Ocean Engineering

Sea Grant

University of Rhode Island

Marine Technical Report No. 16

Kingston 1974

Additional copies of Marine Technical Report Number 16 are available from the Marine Advisory Service, University of Rhode Island, Narragansett Bay Campus, Narragansett, Rhode Island 02882.

CONTENTS

TABLES

FIGURES

Introduction

Knowledge of the behavior of the trawling gear is important in evaluating the performance of a trawler-trawl gear system. Knowing the drag of the trawl gear makes it possible to match gear to a trawler for optimum efficiency or to design an optimum propeller. It also means that it can be determined whether or not a given trawler can tow a new trawl gear at a required speed. A method of calculating this drag is described (as well as a computer model). Use is made of previously developed calculations and experimentally obtained results on the drag of flat panels of fishing netting.

CALCULATION OF TRAWLING GEAR DRAG

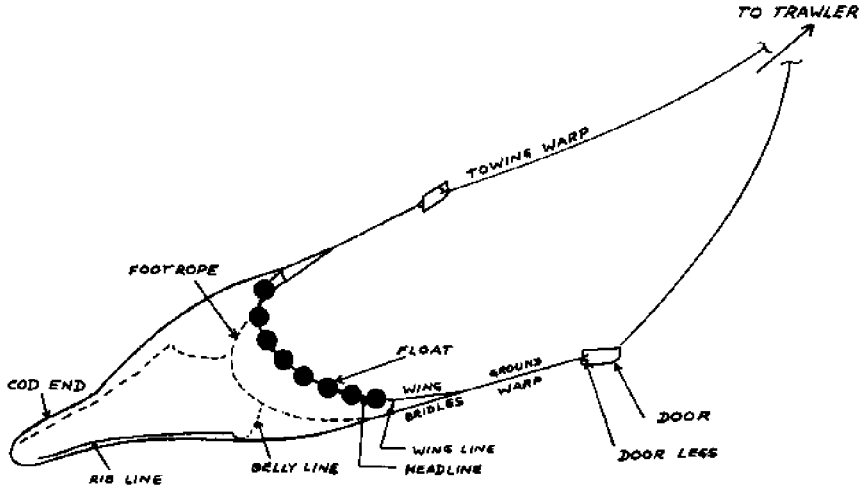

Figure 1. Components of typical trawl gear.

Basis of the Theoretical Model

A typical trawling gear is made up of several components. These are: (1) the net bag; (2) the cod end; (3) lines associated with the net bag which include the wing bridles, bridle lines, rib line, door legs, footrope, headline, and hanging line; (4) ground warps; (5) floats; (6) doors, and (7) towing warps.

These components are shown in figure 1. The total resistance of the trawling gear is assumed to be equal to the sum of the individual resistances of its components. This assumption neglects the effect of interference and component interaction which could make the flow past each component different from the free flow situation. The two main contributors to the total resistance are the doors and the net bag and, since these two are set apart from each other, little or no hydrodynamic interference or interaction between them should exist. Consequently, the error introduced by treating each component separately will only be due to the smaller components, and these contribute a minor portion of the overall resistance.

The drag force acting on the towing warps, however, cannot be calculated as an independent quantity. Since the latter is highly dependent on cable configuration which is, in turn, dependent on the forces acting at the ends of the cables, the analysis of the hydrodynamic resistance of the towing warp requires the solution of the equations of equilibrium for a towed cable. Consequently, the problem is attacked by lumping the first six components of the gear into one body which is attached to one end of the warp and the effect of this body is represented by a force component of known magnitude and direction. The upper end of the warp is fixed to the vessel and the force there is unknown both in magnitude and direction. The application of the equations of equilibrium for a towed cable allows solving for the two unknowns which are then combined with the known force at the trawl end in order to estimate the hydrodynamic drag force acting on the warps of the gear.

Geometry of Nets

Figure 2 shows a typical net panel of n x m meshes and figure 3 shows a typical mesh net. The hanging coefficient of a net is given by

$$\xi = \frac{2L_b - l}{2L_b} \qquad (1)$$

Suppose that a long narrow rectangular strip of webbing n meshes long and m meshes deep is "hung" (joining pieces of netting together and attaching them to the ropes) by a hanging coefficient ξ. Let the net be made of uniform meshes of stretched length $2L_b$. For one mesh, equation 1 gives

$$l = 2L_b - 2L_b\xi$$

$$= 2L_b (1 - \xi)$$

If the total length of the net is l_t then

$$l_t = 2nL_b (1 - \xi)$$

where n is the total number of meshes in the "length" direction. On the other hand, since a mesh is a parallelogram, the "depth" of the net, d_t, can also be found. Let the depth of the mesh opening be denoted by d so that

$$l^2 + d^2 = (2L_b)^2$$

or

$$d^2 = 4L_b^2 - l^2$$

Substituting

$$d = 2L_b\sqrt{(2\xi - \xi^2)}$$

The depth of the net is $d_t = md$

$$d_t = 2mL_b \sqrt{2\xi - \xi^2}$$

where m is the number of meshes in the "depth" direction.

From figure 3

$$\cos\theta = \frac{l}{2L_b} = 1 - \xi$$

and

$$\sin\theta = \frac{d}{2L_b} = \sqrt{2\xi - \xi^2}$$

Thus the angle θ and the hanging coefficient ξ can be used interchangeably.

The surface area of a mesh is given by

$$A_{mesh} = 2L_b^2 \cos\theta \sin\theta$$

The length of the net panel is

$$l_t = 2nL_b (1 - \xi) = 2nL_b \cos\theta$$

The depth of the net panel is

$$d_t = 2mL_b \sqrt{2\xi - \xi^2} = 2mL_b \sin\theta$$

The total number of meshes in a rectangular net is 2mn so that total surface area of a panel is

$$A_{panel} = 2mn\ A_{mesh}$$

or

$$A_{panel} = 4L_b^2\ mn\ \cos\theta\ \sin\theta \qquad (2)$$

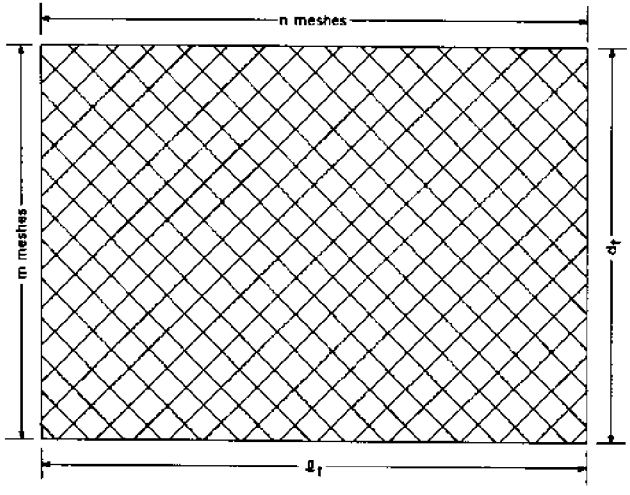

Figure 2. Typical net panel of n x m meshes.

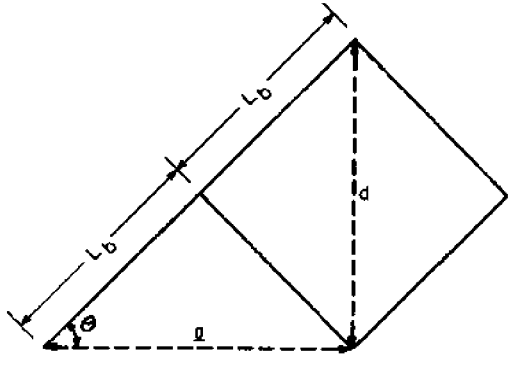

Figure 3. Typical mesh.

Most nets used in the fabrication of trawls are tapered. For this purpose, net manufacturers have established a terminology to indicate the degree of tapering which, in turn, allows one to determine the number of meshes in a tapered net. Figure 4 shows that two sides of a mesh make what is known as a point and the one side of the next mesh which runs in line is called a bar. The cut combining the two is referred to as one point, one bar. This operation would decrease the size of the net by one mesh every six rows. The upper or lower edge of a mesh (clean side) is called a mesh, and the side of the next mesh running in line is known as a bar. The cut combining the two is referred to as one mesh, one bar. Table 1 lists a few of the principal cuts.

Figure 5 shows a uniform sheet of netting which has been cut and used as a trawl panel and its final shape is shown in figure 6. Originally, the panel was a rectangle 188 meshes long and 25 meshes deep. The panel was then cut in a 2B-1P pattern for which Table 1 indicates a loss of 1 mesh in 4 rows. The cut is applied to both sides of the panel so that the actual loss is 2 meshes in 4 rows. Since there are 2m rows in a panel it follows that 50 rows is equivalent to 12-1/2 groups of 4 rows each. Consequently a 2B-1P cut results in a total loss of 25 meshes, and if one starts with 188 meshes at the top of the panel one is left with only 163 meshes along the bottom. The original number of meshes in the panel was 2mn, or 9400, and after the cut is made only 9375 meshes are left.

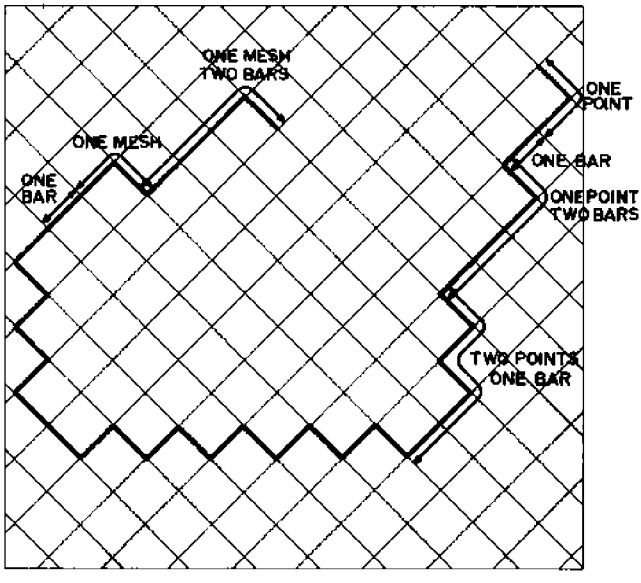

Figure 4. Typical cuts found in nets.

TABLE 1. Principal cuts found in nets.

CUT	LOSS	CUT	LOSS
All Bars	1 Mesh in 2 Rows	1P1B x 2	1 Mesh in 5 Rows
1P4B	1 Mesh in 3 Rows	1P2B	
1P2B	1 Mesh in 4 Rows	1P1B x 3	1 Mesh in 7 Rows
1P1B	1 Mesh in 6 Rows	2P1B	
2P1B	1 Mesh in 10 Rows	1P1B	1 Mesh in 8 Rows
All Points	None	2P1B	
1M1B	1 Mesh in 3 Meshes	2P1B x 3	1 Mesh in 9 Rows
1M2B	1 Mesh in 2 Meshes	1P1B	
		3P1B	1 Mesh in 12 Rows
		2P1B	
		5P1B	1 Mesh in 24 Rows

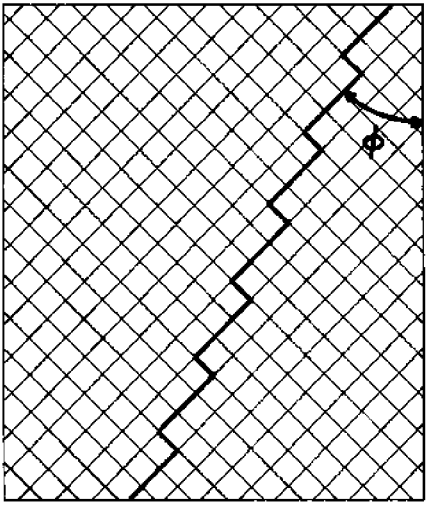

Figure 5. Net panel cut at angle of taper ϕ.

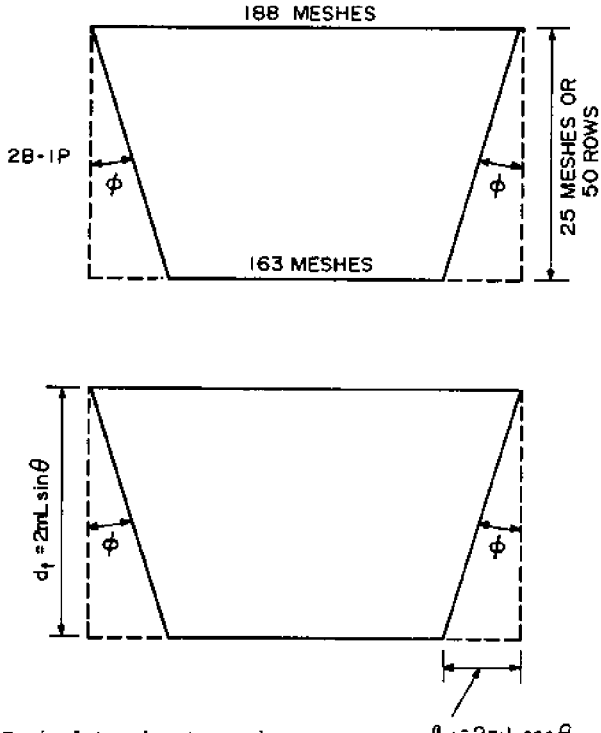

Figure 6. Typical trawl net panel.

The resulting angle of taper, ϕ, can be evaluated as follows. The length of any section of one side of netting is

$$\ell_{ti} = 2n_i L_b \cos\theta$$

where n_i is the number of meshes lost on each side as shown in figure 6. The depth of the netting panel remains unchanged and is given by

$$d_t = 2m\ L\ \sin\ \theta$$

From figure 6 the angle of taper is given by

$$\phi = \tan^{-1} \frac{\ell_{ti}}{d_t}$$

or

$$\phi = \tan^{-1} \frac{2n_i L_b \cos\theta}{2mL_b \sin\theta}$$

which reduces to

$$\Phi = \tan^{-1} \frac{n_i}{m} \cot \theta$$

In the case of the panel of figure 6

$$n_i = \frac{188 - 163}{2} = 12.5$$

and if m = 25 meshes and $\theta = 60^{\circ}$,

$$\Phi = \tan^{-1} \frac{12.5}{25} \cot 60^{\circ} = 16^{\circ}$$

The average solidity, S, of a net bag made up of more than one mesh size can be calculated from

$$S = \frac{s_1 q_1 + s_2 q_2 + \cdots + s_n q_n}{Q} = \frac{\sum_{i=1}^{i=N} s_i q_i}{Q} \qquad (3)$$

where s_i is the solidity of the ith panel, q_i is the number of meshes in the ith panel, and Q is the total number of meshes in the entire bag. The panels of a net bag will have various shapes or combinations of shapes. Figure 7 shows the most commonly encountered geometries. For example, if a net bag has two panels of shape A, one panel of shape B, two panels of shape C, and two panels of shape D, the average solidity S can be computed as follows. Panels A, B, and C of figure 7 are made of 5-inch mesh nets and panels D are made of 4.5-inch mesh nets. The number of meshes in each panel A is

$$q = (2 \times 50 \times 10) + (50 \times 50)$$
$$= 3,500 \text{ meshes}$$

and two panels will have 7,000 meshes. The number of meshes in panel B is

$$q = (2 \times 27 \times 140) + (2 \times 27 \times 20)$$
$$= 8,640 \text{ meshes}$$

The number of meshes in each panel C is

$$q = (30 + 45) \times \frac{2 \times 80}{2} = 6,000 \text{ meshes}$$

and two panels will have 12,000 meshes. The total number of 5-inch meshes is

$$q_i = 7,000 + 8,640 + 12,000$$
$$= 27,640 \text{ meshes}$$

The solidity s_i of the ith panel is given by

$$s_i = \frac{(2L_b D_b) + (\pi D^2 K)}{2L_b^2 \cos\theta \sin\theta}$$

In the case of the 5-inch mesh net panels the solidity is

$$s_i = [(2 \times 2.5 \times 0.1) + (3.1416 \times 0.3 \times 0.3)]/$$
$$[2 \times (2.5)^2 \times 0.5 \times 0.866]$$
$$= 0.1054$$

where $\theta = 60^o$, $L_b = 2.5$ inches, $D_b = 0.1$ inch and $D_k = 0.3$ inch.

The number of meshes in panels D is

$$q_2 = (2 \times 80 \times 40) + (2 \times 50 \times 80)$$
$$= 14,400 \text{ meshes}$$

and two panels will have 28,800 meshes.
The solidity of panels D is

$$s_2 = [(2 \times 2.25 \times 0.1) + \frac{(3.1416 \times 0.3 \times 0.3)}{4}]/$$
$$[2 \times (2.5)^2 \times 0.5 \times 0.866]$$
$$= 0.1188$$

where $\theta = 60^o$, $D_b = 0.1$ inch, $L_b = 2.25$ inches, and $D_k = 0.3$ inch.
The total solidity, S, of the net bag is

$$S = \frac{s_i q_i + s_2 q_2}{Q}$$
$$= \frac{(0.1054 \times 27,640) + (0.1188 \times 28,800)}{(27,640 + 28,800)}$$
$$= 0.1121$$

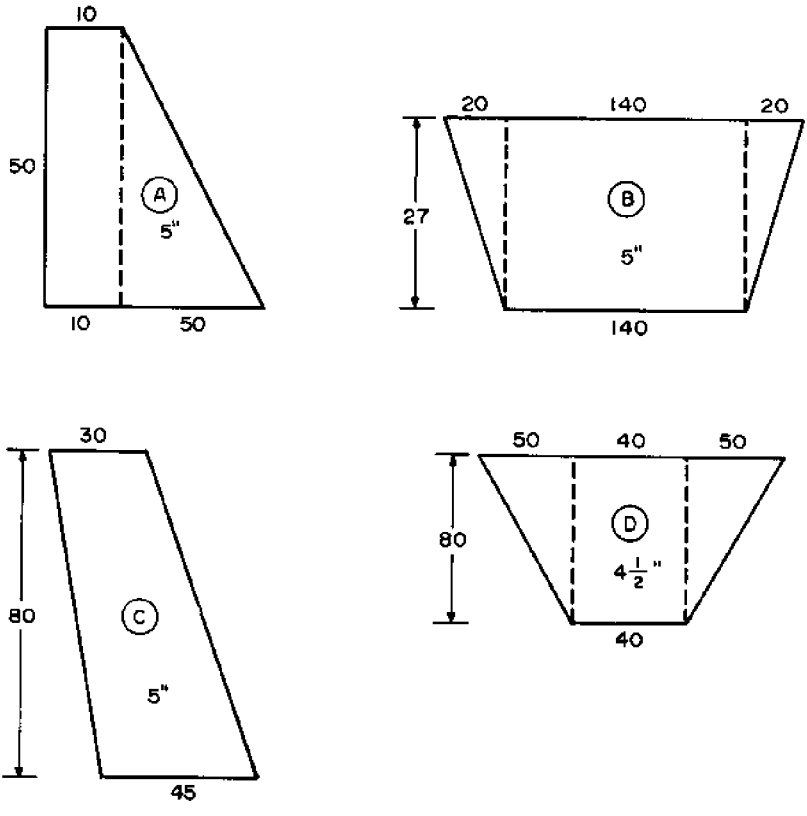

Figure 7. Common panel geometries.

Empty Area Between the Wings of a Yankee 35

The size of the empty area between the wings of a trawl net can be estimated from the geometry of the top and bottom panels. Figure 8 shows the portion of the top panel containing the wings. The area between the wings is given by

$$
\begin{aligned}
A_{\substack{\text{empty} \\ \text{top}}} &= (2n_t l_b \cos\theta + 2n_b l_b \cos\theta) \times m l_b \sin\theta \\
&= (n_t + n_b)\ 2 \cos\theta \sin\theta\ l_b^2 \\
&= (160 + 60) \times 2 \times 0.5 \times 0.866 \times (2.5)^2 \\
&\approx 48{,}800 \text{ in}^2
\end{aligned}
$$

Figure 9 shows the portion of the bottom panel containing the wings. In this case one must first find the angle ϕ_n which in turn gives AB and CD. From Figure 9 the angle α is given by

$$\alpha = \tan^{-1} \frac{2 \times 50 \times 2.25 \times 0.5}{2 \times 80 \times 2.25 \times 0.866}$$

$$= \tan^{-1} 0.36$$

$$= 20^{\circ}$$

The angle ϕ_n is then given by

$$\phi_n = 90^{\circ} - \alpha$$

$$\phi_n = 70^{\circ}$$

The next step is to find the distance EF or GH. From triangle BEF,

$$\tan\phi = \frac{BF}{EF} = \tan 70^{\circ}$$

and

$$EF = \frac{2 \times 80 \times 2.5 \times 0.866}{2.7475} = 126.3 \text{ inches}$$

It follows that

$$GF = GH + HE + EF$$
$$= HE + 2EF$$

where

$$HE = 2 \times 140 \times 2.25 \times 0.5 = 315 \text{ inches}$$

then

$$GF = 315 + 2(126.3) = 567.6 \text{ inches}$$

and

$$CD = AB - (AC + BD) = GF - (AC + DB)$$
$$CD = 567.6 - [(2 \times 30 \times 2.5 \times 0.5) \times 2]$$
$$CD = 417.6 \text{ inches}$$

Likewise,

$$JK = HE - (HJ + KE)$$

where

$$HJ = 2 \times 45 \times 2.5 \times 0.5 = 112.5$$

and

$$HJ = KE$$

so

$$JK = 315 - (112.5 + 112.5) = 90 \text{ inches}$$

It follows that the area between the wings in the bottom panel is given by

$$A_{\substack{empty \\ bottom}} = (CD + JK) \times \frac{BF}{2}$$

where

$$BF = 2 \times 80 \times 2.5 \times 0.866 = 346.4 \text{ inches}$$

and

$$A_{\substack{empty \\ bottom}} = (417.6 + 90) \times \frac{346.4}{2}$$
$$= 87,916 \text{ in}^2$$

The total empty surface area between the wings of the trawl is approximately

$$A_{\substack{empty \\ total}} = A_{\substack{empty \\ top}} + A_{\substack{empty \\ bottom}}$$
$$= (48,800 + 87,916) \text{ in}^2$$
$$\approx 950 \text{ ft}^2$$

Maximum and Minimum Angles of Attack of a Yankee 35

Figure 10 shows a schematic of the cone containing the approximate shape of the trawl net ahead of the cod end. The angle α_1 is the minimum angle of attack of the net and the angle α_2 is the maximum angle of attack.

The approximate magnitudes of these angles are

$$\alpha_1 = \tan^{-1} \frac{b}{h} = \tan^{-1} \frac{3.4}{80}; \quad \alpha_1 \approx 2.5^\circ$$

and

$$\alpha_2 = \tan^{-1} \frac{a}{h} = \tan^{-1} \frac{14}{80}; \quad \alpha_2 \approx 10^\circ$$

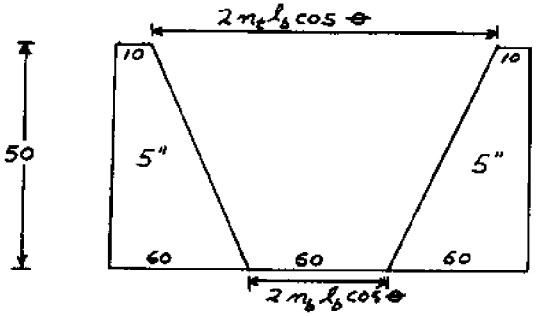

Figure 8. Portion of the top panel of a Yankee 35 containing the wings.

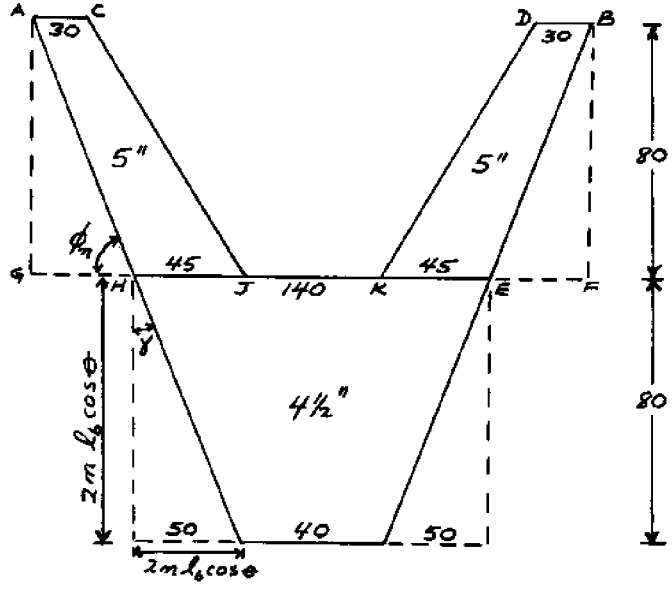

Figure 9. Portion of the bottom panel of a Yankee 35 containing the wings.

Drag Force Acting on the Net Bag

The net bag can be approximated by a conical net with an elliptical mouth, where the major axis of the ellipse is given by the wingspread, 2a, and the minor axis by the headline height 2b. Field measurements on bottom trawls show that headline height and wingspread remain essentially constant in the range of speeds of interest. The equation developed in

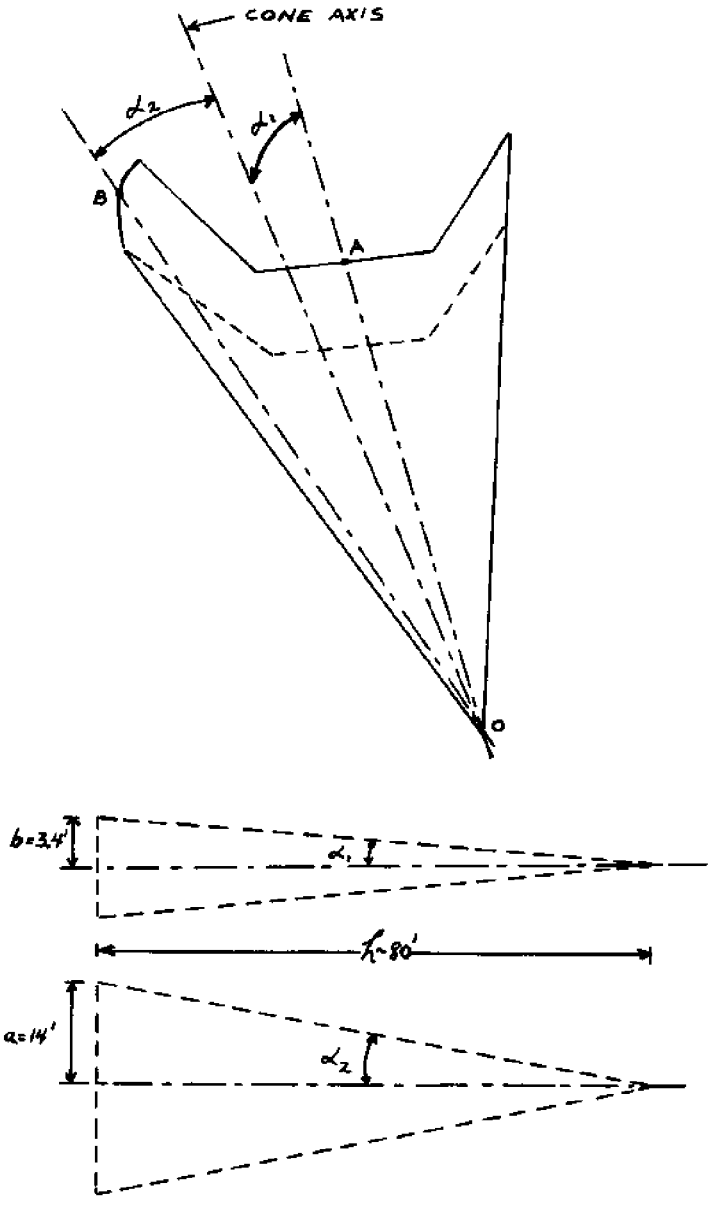

Figure 10. Maximum and minimum angles of attack of a Yankee 35 trawl.

reference 2 indicates that the drag force acting on a conical net with a circular opening is directly proportional to the area of the mouth opening.

$$D_{cone} = C_{D90^\circ} \frac{1}{2} \rho V^2 S \pi r^2 \quad (4)$$

Assuming that the same is true for the net with an elliptical opening, the drag force on this net can be approximated by

$$D_{cone} = C_{D90^\circ} \frac{1}{2} \rho V^2 S \pi ab \quad (5)$$

where C_{D90° = drag of flat net panel of required mesh

S = solidity ratio, defined by equation 3

Figure 11 shows the layout of the top and bottom sections that make up the bag. Each section is typically made up of panels of different shape, size, and mesh size. The mesh size does not differ much from panel to panel in bottom trawls and, consequently, the coefficient of drag, C_{D90°, is assumed to be constant throughout the bag. The solidity, S, of the net will vary as the mesh size changes. Thus, an average solidity must be computed using equation 3. The twine diameter, D_b, is given by the empirical relationship

$$D_b = k^* (N_t)^{1/2}$$

where N_t is the Tex Number in gm/km and k* is a constant depending on the twine material, with a typical value of 0.05. The knot diameter, D_k, is taken to be approximately three times the twine diameter based on actual observations.

The coefficient of drag, C_{D90°, and solidity, S, can be computed, and the headline height, 2b, and the wingspread, 2a, can be estimated from available experimental data. With these four values the total drag force acting on a bottom trawl at a given speed V can be computed using equation 4 or 5.

The representation of the net bag by a conical net is only an approximation since the portion corresponding to the apex region of the cone is absent in the case of the real gear. However, the presence of the cod end can be taken to act as a rounded closure, replacing the pointed apex, and thus the conical shape would seem to be a reasonably good approximation. The presence of the wings in a trawl net can be represented by considering the conical net as having two portions of its surface removed. These portions correspond to the "empty" areas between the wings in the top and bottom panels of the net.

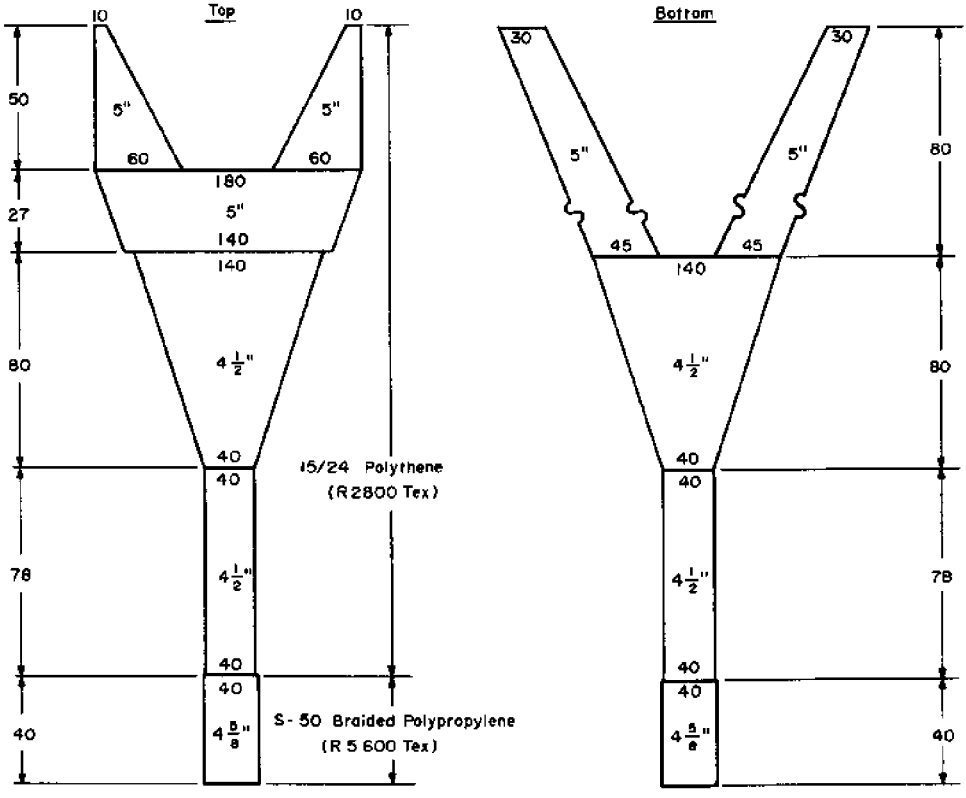

Figure 11. Top and bottom views of a Yankee 35 trawl.

Consequently, the effect of the wings on the total drag force acting on the conical net should be a reduction in the drag force due to the missing area. If the conical net were circular, all portions of the net would be inclined at the same angle with respect to the flow. However, in the more realistic case of an elliptical cone, the angle will vary continuously.

Figure 10 shows a conical net with wings. It can be seen that portions of the wings lie in different planes and, consequently, their inclination to the flow is not constant throughout. Therefore, when applying a correction to the drag force acting on a complete conical net, two effects must be taken into consideration. These are the reduction in area and the variation in angle

of attack of the remaining wings. The computation of the empty surface area between the wings of a Yankee 35 trawl has been given before.[2] The total surface area of the empty portion is about 950 feet^2. If the conical net were circular then the drag force computed from equation 4 would have to be reduced by the amount corresponding to the missing area. However, the Yankee 35 (and most other trawls) have elliptical mouths and the effect of variation in the wing angle of attack must also be accounted for when computing the drag force. Figure 10 shows that the angles of attack associated with the empty portion of the net are smaller than those associated with the wings. The angle between the longitudinal axis of the cone and line OA is α_1 and the wings at an angle α_2. The magnitude of these two angles can be estimated from the approximate configuration of the trawl as it moves through the water. For the Yankee 35 trawl values obtained are $\alpha_1 \sim 2.5^\circ$ and $\alpha_2 \sim 10^\circ$. Now if the empty portions contained netting panels, their coefficient of drag would be approximately $C_{D90} \sin \alpha_1$. Similarly the coefficient of drag of the wings is $C_{D90} \sin \alpha_2$ as an average. Consequently, the drag force that would be exerted on the empty portions if these contained netting would be

$$D_{\substack{\text{empty} \\ \text{portions}}} = C_{D90^\circ} \sin \alpha_1 \; 1/2 \; A_{\substack{\text{empty} \\ \text{portion}}} \; \rho v^2 S$$

Similarly the drag force exerted on the overall cone is

$$D_{cone} = C_{D90^\circ} \; 1/2 \; v^2 S \; \pi \; ab$$

The ratio of the drag force which would act on the empty portions, if they contained netting, to that of the overall cone is

$$\frac{D_{\text{empty portion}}}{D_{cone}} = \frac{\sin \alpha_1 \; A_{\text{empty portion}}}{\pi \; ab} = k_1$$

since ρ, V and S are the same for both. With $\alpha_1 \sim 2.5^\circ$, $A_{\text{empty portion}} = 950$ ft.^{2}, a = 14 ft., and b = 3.4 ft., the value of k_1 is about 0.30. Consequently, the drag force acting on a conical net with wings is given by equation 5 reduced by a factor $(1-k_1)$. Equation 5 then becomes

$$D_{cone} = C_{D90^\circ} \; 1/2 \rho v^2 \; S \pi \; ab \; (1-k_1)$$

In the case of the Yankee 35 the drag force acting on the conical portion should be reduced by 30 percent.

Drag Force Acting on the Cod End

The cod end of a trawl acts as a container for the fish until the trawl is removed from the water. The cod end has the shape of a cylindrical net with one side opened and one side closed. Since the longitudinal axis of this cylindrical body is parallel to the flow, the panels of netting that make up the cod end will have a zero angle of attack. Accordingly, the coefficient of drag for zero angle of attack is given by frictional effects only and these are very small. Consider the cod end as an empty cylinder of length l_c and diameter d_c, then a Reynolds number can be defined based on l_c as $N_r = \frac{Vl_c}{\nu}$.

Hoerner (1965) gives values of the coefficient of frictional drag C_f for hollow cylinders as a function of their aspect ratio l/d and the Reynolds number as defined above. Since the definition of the coefficient C_f is based on wetted surface area, the total frictional drag force D_f for the empty cod end (hollow cylinder) is given by

$$D_f = \frac{C_f (\rho V^2) A_s}{2}$$

where A_s is the wetted surface area of the cod end and it is calculated from the geometries of the knots and the bars that make up the net. The wetted surface area of one bar is given by

$$A_{s_b} = \pi (L_b D_b)$$

and the wetted surface area of one knot is given by

$$A_{s_k} = \pi D_k^2$$

The number of meshes that make up the cod end is M, the total number of bars, B, and the total number of knots, K. Consequently, the total wetted surface area of the cod end, A_s, is given by

$$A_s = B \pi (L_b D_b) + K \pi D_k^2$$

The total frictional drag force acting on the empty cod end is

$$D_f = \frac{C_f (\rho V^2) [B \pi (L_b D_b) + K \pi D_k^2]}{2}$$

For typical cod end lengths and trawling speeds the Reynolds number is at least 10^7. Hoerner (1965) gives values of C_f for an approximate aspect ratio l/d of ten as about 0.0005. When a cod end is filled with fish, it is considered as a solid cylinder of length l_c and diameter d_c. The drag force acting on it will now have an additional component which is the viscous pressure drag caused by boundary layer separation. Hoerner (1965) gives the coefficient of drag for a cylindrical body in axial flow with blunt shape. The coefficient of drag C_D has a constant value of about 0.82 for ratios l/d of 2.0 and above. In the real situation of the cod end, the length l of the solid cylinder will vary as the cod end becomes filled with fish. This however, should not affect the magnitude of C_D beyond a l/d ratio of 2. There will be a variation of drag according to the portion of cod end that is empty.

Assuming than an $l/d \geq 2$ is achieved relatively fast in a typical fishing operation the coefficient of drag for the solid portion, C_D, can be taken to be 0.82 for typical cod ends.

If the cod end becomes filled with fish at a rate, r, then the length of the portion that is filled at any time, t, is given by $l = rt$. Further, let n be the ratio of filled length, l, to total cod end length, l_c, i.e. $n = l/l_c$. The total drag force acting on the cod end at any particular time after fill up has started becomes

$$D_{\substack{\text{cod}\\\text{end}}} = D_{\substack{\text{filled}\\\text{portion}}} + D_{\substack{\text{empty}\\\text{portion}}}$$

or

$$D_{\substack{\text{cod}\\\text{end}}} = 0.82 \left(\frac{\rho V^2}{2}\right) \left(\frac{\pi}{4} d_c^2\right) n_1 \qquad \begin{matrix} n_1 = 0 \text{ for } t = 0 \\ n_1 = 1 \text{ for } t > 0 \end{matrix}$$

$$+ C_f \left(\frac{\rho V^2}{2}\right) [B \pi (L_b D_b) + K \pi D_k^2] (1-n)$$

Before the beginning of fill-up the total drag is given only by the second term on the right hand side of the above equation. The first term or the drag due to pressure will be zero under these circumstances.

Drag Force Acting on the Lines Associated with the Net Bag

The drag force acting on all the lines associated with the net bag can be calculated from the cross flow principle (Hoerner 1965) which is applicable to cylindrical cables inclined at an

angle ϕ to the flow. Thus, the total drag acting on any of the net bag lines is given by

$$D_{\substack{\text{ground}\\\text{warps}}} = (C_{D_{basic}} \sin^3\phi + \Delta C_D) \left(\frac{\rho V^2}{2}\right)(d_1 \ell_1) + D_F$$

where d_1 is the line diameter and ℓ_1 is cable length. In the range of Reynolds numbers of interest $C_{D_{basic}}$ is taken as 1.10 and ΔC_D as 0.02. $C_{D_{basic}}$ is the coefficient of drag for a cable which is perpendicular to the flow and ΔC_D is the frictional component which is added to the term involving the $\sin^3 \phi$ term in order to match experimental results. The angle ϕ can be estimated from the geometry of the trawl. D_F is the ground friction force acting on the footrope and it has to be determined experimentally.

Drag Force Acting on the Ground Warps

The ground warps are lines that connect the net bag to the doors. They are much longer cables than those associated with the net bag. However, the total drag force is also computed by the application of the cross-flow principle and it is given by

$$D_{\substack{\text{ground}\\\text{warps}}} = (C_{D_{basic}} \sin^3\omega + \Delta C_D) \left(\frac{\rho V^2}{2}\right) (d_g \ell_g)$$

where d_g is the ground warp diameter, and ℓ_g is the ground warp length. The angle ω which the ground warp forms with the direction of the flow is found from the approximate configuration adopted by the trawl as it is towed through the water. As before, $C_{D_{basic}}$ is 1.10 and ΔC_D is 0.02.

Drag Force Acting on the Floats

The floats attached to the headline of the trawl usually consist of cast aluminum spheres. The drag force acting on n_f floats is given by

$$D_{floats} = n_f C_{D_{fl}} \left(\frac{\rho V^2}{2}\right) \left(\frac{\pi d^2_{fl}}{4}\right)$$

where d_{fl} is the diameter of the float and the drag coefficient is C_{Dfl} for a spherical float. For typical values of Reynolds number C_{Dfl} is taken as 0.47 (Hoerner 1965).

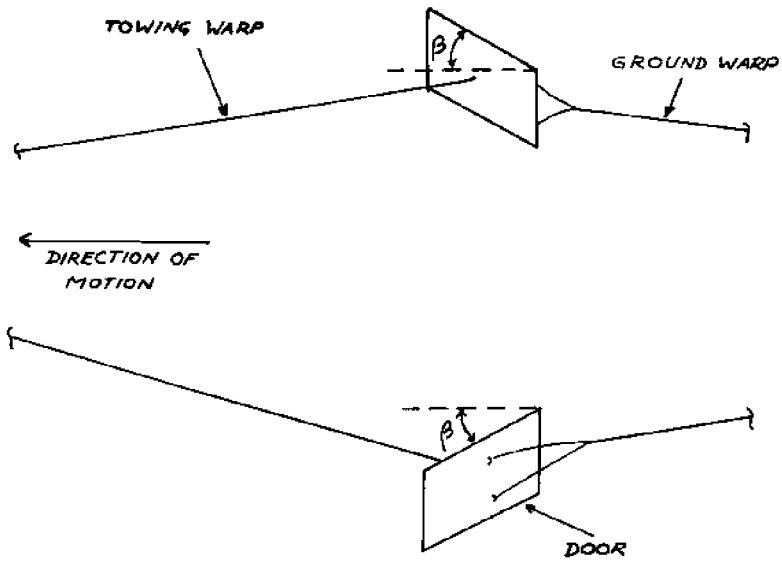

Figure 12. Trawling gear doors inclined at an angle β with respect to the direction of motion.

Resistance Force Acting on the Doors

The doors used by most trawls are flat plates. These act at an angle of attack β with respect to the flow as shown in figure 12. The doors, also are tilted in the transverse and vertical directions but experimental measurements show that the hydrodynamic drag coefficient is not significantly affected by these angles (Crewe, 1964). In bottom trawls the doors touch the bottom, and consequently, the resistance to motion due to bottom friction must be considered in addition to the hydrodynamic drag.

The total hydrodynamic drag coefficient, C_{DT}, for any lifting surface which is inclined to the flow can be expressed as

$$C_{DT} = C_{Di} + C_{D_P} + C_{D_f}$$

where C_{Di} is the induced drag coefficient, C_{D_P} is the pressure drag coefficient, and C_{D_f} is the frictional drag coefficient.

The value of C_{DT} for a flat plate can be obtained directly from experimental data as a function of the angle of attack β. Hoerner (1965) gives a curve showing the normal force coe-

fficient C_N as a function of β. That curve can be represented by the equations

$$C_N = 0.04\ \beta^\circ \quad 0 < \beta \leq 45^\circ \quad \text{or} \quad C_N = 1.17,\ 45^\circ \leq \beta \leq 90^\circ$$

The total coefficient of drag C_{DT} is the component of C_N in the direction parallel to the flow and is given by

$$C_{DT} = C_N \sin \beta$$

or

$$C_{DT} = 0.04\ \beta^\circ \sin \beta,\ 0 < \beta \leq 45^\circ$$

and

$$C_{DT} = 1.17 \sin \beta,\ \ 45^\circ \leq \beta \leq 90^\circ$$

The total drag force acting on a door, D_D, is then given by

$$D_D = C_{DT} \left(\rho \frac{V^2}{2}\right) A_D \qquad (6)$$

where A_D is the frontal area of the rectangular door.

The door resistance due to bottom friction can be estimated from available field measurements (Crewe, 1964) on rectangular doors. There are two types of forces that arise when the doors touch the bottom. The first type is the ground friction tangential force acting parallel to the doors. These are the forces that will add to the total door resistance. The second type is theground reaction force acting sideways and upward, perpendicular to the doors. Figure 13 shows the friction and reaction forces when a door is heeled in and when a door is heeled out. Crewe (1964) conducted measurements of these forces employing specially instrumented doors. Load cells were installed to measure the two types of forces mentioned before. The upward component of ground reaction was found to be about 30 percent of the weight of the door in water while the sideways component of ground reaction was found to be about 50 percent. The ground shear or friction forces seemed to be more significant on muddy bottoms than on hard bottoms. Figure 14 shows a plot of ground friction and reaction forces versus trawling speed. The effects of angle of heel on the total coefficient of drag C_{DT} have been investigated by Crewe. These tests indicated that the total coefficient of drag did not vary significantly over a range of angles of heel between -20° and $+20^\circ$. Since this is the typical range encountered in trawling operations, it can be safely assumed that C_{DT} will remain constant.

The total resistance, R_D, can now be computed by adding the hydrodynamic drag, D_D, and the bottom frictional resistance, R_f,

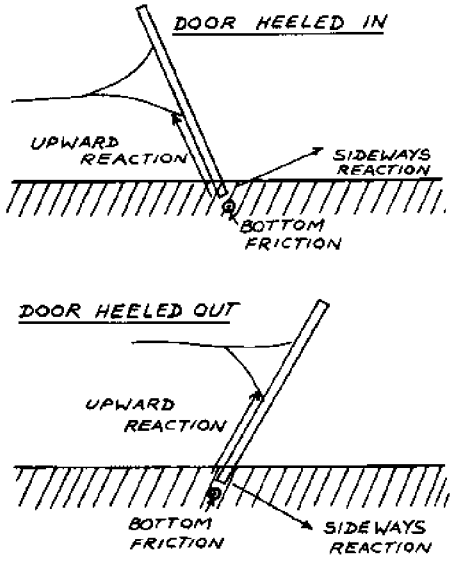

Figure 13. Friction and reaction forces exerted by the ocean bottom on trawling gear doors.

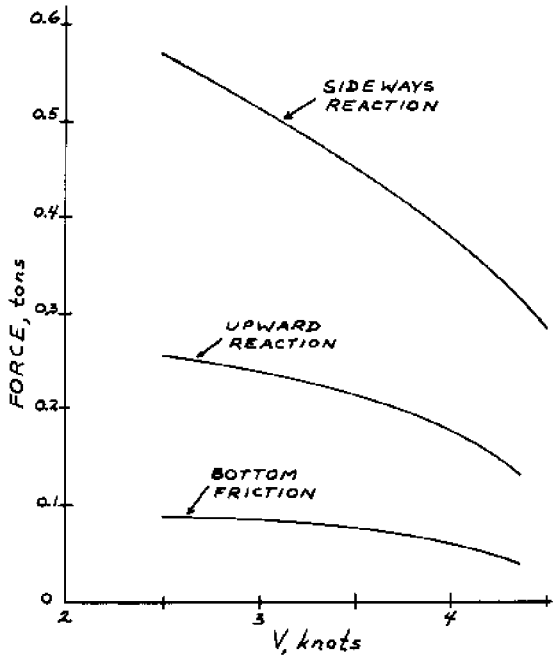

Figure 14. Friction and reaction forces vs. trawling speed for typical bottom trawl doors (ref. 2).

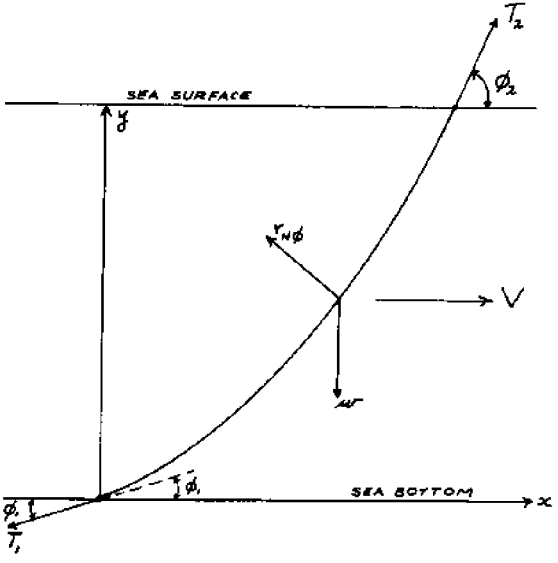

Figure 15. Towing warp forces and configuration during trawling.

$$R_D = D_D + R_f$$

The value of R_f is obtained from figure 14 and D_D can be found from equation 6. The doors used in these experiments had dimensions similar to those used by the Point Judith trawler fleet. However, there is still need to conduct more tests on doors of various geometries and sizes, acting over different types of bottom soils, in order to better understand the interaction between door and soil as a function of speed.

Drag Force Acting on the Towing Warps

The drag force acting on a towing warp is a function of its shape which, in turn, is determined by the system of forces acting on it.

Figure 15 shows the forces and geometry of a warp during trawling. T_1 and T_2 are the tensions at the warp ends; point 1 represents the trawl and point 2 represents the vessel; w is the weight per unit length of cable in water and $r_{N\Phi}$ is the hydrodynamic force per unit length of cable.

The hydrodynamic force coefficient, $C_{N\Phi}$, of a straight circular cable inclined at an angle Φ to the flow is given by

$$C_{N\Phi} = C_{D_{basic}} \sin^2 \Phi$$

where $C_{D_{basic}}$ is the hydrodynamic drag coefficient for a circular cable perpendicular to the flow and $C_{N\Phi}$ is the hydrodynamic force coefficient in the direction normal to the cable longitudinal axis. Figure 16 shows the forces associated with these coefficients. L is the force in the vertical direction and D is the hydrodynamic force or drag in the horizontal direction. The real situation of a towing warp is shown in figure 17 where a small element of curved cable of length d_{lw} is shown. The tension forces at each end of the element are given by T and (T + dT). The weight in water of the cable element is wdl_w. The differential hydrodynamic force, $dR_{N\Phi}$, acting on the cable element is given by

$$dR_{N\Phi} = C_{N\Phi} \left(\frac{\rho V^2}{2}\right) d_w dl_w$$

and

$$dR_{N\Phi} = C_{D_{basic}} \left(\frac{\rho V^2}{2}\right) \sin^2 \Phi \, d_w dl_w$$

Assuming that the element of cable shown in figure 17 is a small circular arc, the equations of equilibrium for the forces acting on the element can be set up.
These are

$$-T\cos\frac{d\Phi}{2} + (T + dT)\cos\frac{d\Phi}{2} - wdl_w \sin\left(\Phi + \frac{d\Phi}{2}\right) = 0$$

in the tangential direction, and

$$dR_{N\Phi} + \sin\frac{d\Phi}{2} + (T + dT)\sin\frac{d\Phi}{2} - wdl_w \cos\left(\Phi + \frac{d\Phi}{2}\right) = 0$$

in the normal direction.

The above equations have been solved numerically by Pode (1951). Knowing the tension force and its direction at one end of the cable, the tension force and its direction at the other end can be calculated. Figure 15 is a free body diagram showing the towing warp and a coordinate system which has been defined to comply with Pode's analysis. It is assumed that the cable lies in the vertical x-y plane, parallel to the direction of motion. In the real situation there is an angle between the plane of the cable and the plane of motion, but the angle is small and its effect can be neglected. The magnitude of this

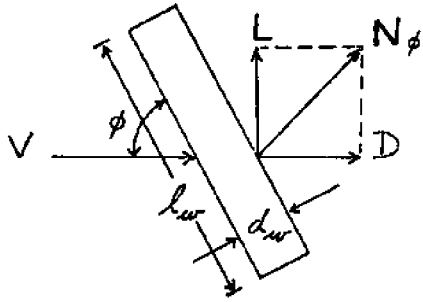

Figure 16. Hydrodynamic forces acting on a towing cable.

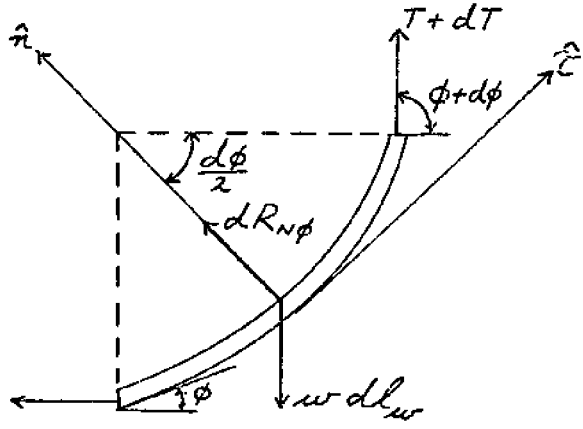

Figure 17. Differential element of a towing cable.

angle can be estimated from the length of the towing warp and the horizontal opening of the trawl mouth. Typically, the towing warp is about 450 feet and the horizontal mouth opening is about 14 feet. In trawling operations the ratio of warp spread to warp length is about 0.7. This gives an approximate spread of 315 feet and an angle of $\tan^{-1}$ (14/315) or 2-1/2° between the plane of the cable and the plane of motion. Consequently, the cable can be assumed to lie in the x-y plane. However, if the trawl in question were not a Yankee 35 design, but one where the half mouth opening is about 40 feet, then $\tan^{-1}$ (40/315) = 7.5°. This angle can no longer be considered negligible and the towing warp cannot be assumed to lie in the x-y plane only. In these cases the equation of equilibrium must include the additional components of forces in the second plane of the warp. The solution will yield a different magnitude for warp tension and, consequently, a different value of towing warp drag.

The drag force, D_w, acting on the cable can be expressed as the difference between the horizontal component of warp tension at the door, T_{1x}, and the horizontal component of warp tension at the vessel, T_{2x}.

$$D_w = T_{2x} - T_{1x}$$

$$T_{1x} = T_1 \cos\phi_1$$

and

$$T_{2x} = T_2 \cos\phi_2$$

The magnitude of T_1 and ϕ_1 can be determined from the known forces acting on the doors. However, T_2 and ϕ_2 are unknown and their magnitudes are found by combining T_1 and ϕ_1 with the equations of equilibrium.

Figure 15 shows that the warp tension at the doors, T_1, is directed along a tangent to the cable. The force T_1 can be split up into two components, T_{1x} and T_{1y}, as shown in figure 18. The horizontal component, T_{1x}, is made up of two terms. The first term is the contribution of the drag force acting on the net bag, the lines associated with it, the ground warps and the floats. This term was defined as D_T. The trawling gear has two doors so that the contribution to one door by D_T will be 1/2 D_T. The second term includes the hydrodynamic resistance and bottom friction acting on the door, R_D. The vertical component, T_{1y}, can be expressed as a sum of three terms. The first term is the weight of the door in the water, W_D. The second term is the vertical component of the hydrodynamic door resistance, D_{Dy}, which depends on the angle of heel of the door. The third term is the vertical ground reaction, N_G. T_{1x} and T_{1y} can now be expressed as

$$T_{1x} = \frac{1}{2} D_T + R_D$$

and

$$T_{1y} = W_D + D_{Dy} - N_G$$

The sign convention used for T_{1y} can be best understood by looking at the free body diagram of a door as shown in figure 19. The tension T_1 acting on the warp at the door end can be written in terms of the horizontal and vertical components as

$$T_1 = (T_{1x}^2 + T_{1y}^2)^{1/2}$$

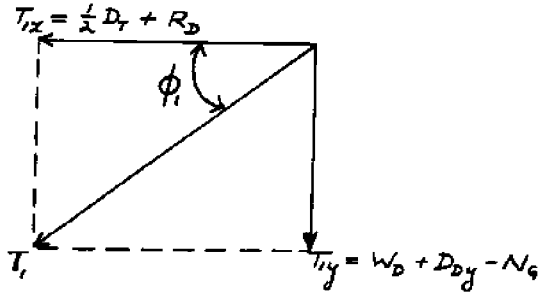

Figure 18. Components of towing warp tension at a door.

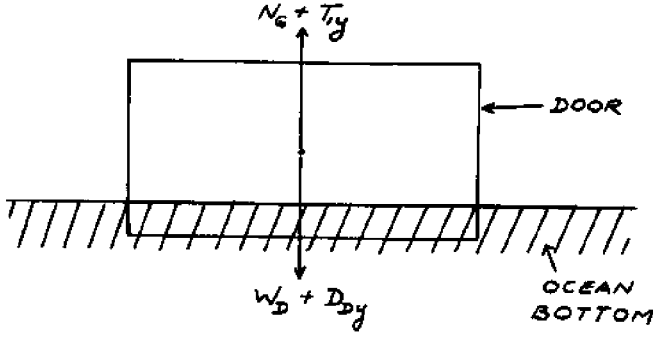

Figure 19. Vertical forces acting on a bottom trawl door.

or $$T_1 = [(\tfrac{1}{2} D_T + R_D)^2 + (W_D + D_{Dy} - N_G)^2]^{1/2}$$

The angle Φ at the door is then given by

$$\Phi_1 = \tan^{-1} \frac{T_{1y}}{T_{1x}}$$

or

$$\Phi_1 = \tan^{-1} \frac{(W_D + D_{Dy} - N_G)}{(\frac{1}{2} D_T + R_D)}$$

The next step in estimating the drag force acting on the towing warps is to find the magnitudes of the tension T_2 and the angle Φ_2 at the vessel end, by means of the equilibrium equations. The procedure to be followed in finding the two unknowns is given by Pode (1951) and is described in the Appendix. With T_1, T_2, Φ_1, and Φ_2 known, the drag force acting on the towing warps can now be calculated.

COMPARISON OF RESISTANCE PREDICTION WITH FIELD MEASUREMENTS ON FULL-SCALE TRAWLING GEAR

The developed equations and procedures have been merged into a computer program which is described in detail in the Appendix. The program was written specifically for the case of Yankee 35 trawling gear and the results of the computation are shown in figure 20. The experimental points corresponding to field measurements lie above the curve drawn on the basis of the theoretical prediction. There are several important reasons for this discrepancy.

The theoretical analysis presented in the previous section does not consider the interaction between the many components of the gear and its effect on the overall resistance characteristics of the trawl. It is quite possible that this interaction is of such a nature that it causes an increase in the hydrodynamic drag of the system. The interaction between two or

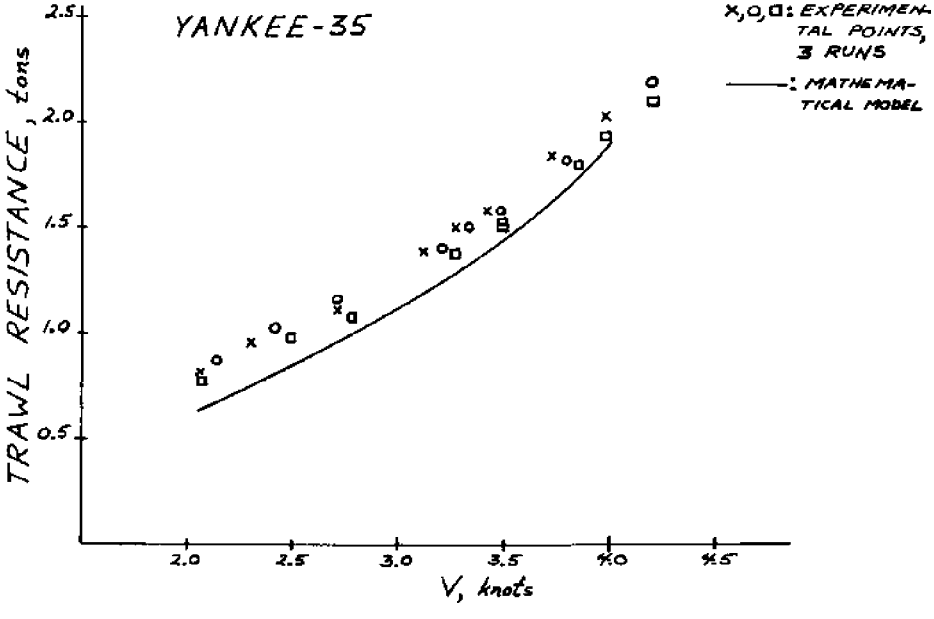

Figure 20. Resistance vs. trawling speed for a Yankee 35 bottom trawl.

more bodies joined together gives rise to interference drag. This drag is usually greater than the sum of the drag forces acting on the individual bodies in free flow. The estimate of the magnitude of this effect by theoretical means is quite complicated and, to the author's knowledge, methods of solution which yield realistic values have not been developed. One possibility would be to test models of conical nets with and without gear attached to them. If separate tests are conducted on this gear, then the difference between the drag estimated simply by adding the drag of the individual components and that measured for the nets with gear attached to them could be established. The effect could be quantified in the form of a ratio of the latter to the former, and the ratio could be applied to the full-scale drag estimate.

In addition to the effect mentioned above, there are two other factors which could possibly affect the magnitude of the drag force acting on a net. One of these is the oscillation of the bars of a mesh due to the shedding of Karman vortices. The alternating shedding of vortices from the two points of separation on the surfaces of a bar produces transverse forces on the bar and causes it to oscillate. If the frequency of vortex shedding is in resonance with the natural frequency of the bar, the bar will deflect excessively.

The second factor to consider is the geometry of the net bag itself. In the development of the resistance model the bag was approximated by a conical net with straight generators. In practice this is not quite the case. The inclination of the surface of the net bag varies along its length, the angles in the forward portion being somewhat larger than those in the after portion. Consequently, the assumption of a constant angle is only an approximation.

When treating the problem of the hydrodynamic drag acting on the footrope, the contribution to the resistance by the gear which is attached to the footrope is not included in the analysis. This requires a good deal of experimental measurements in order to determine the frictional resistance caused by the motion of this gear over the bottom of the ocean. The problem is further complicated by the lack of resistance data for doors acting on the same type of bottom soil as that encountered in the field measurements of the Yankee 35 trawling gear. Since the effect of bottom friction is a large component of total resistance this could be a significant source of error.

Finally, another source of error could very well be the influence of the proximity of the bottom on the frictional resistance of the trawl. Between the bottom of the ocean and the bottom of the trawl, the channeling effect of the water must in-

crease its velocity, at the same time decreasing its pressure. This produces increased friction due to higher flow rate. All of these factors are believed to add up, the net result being a higher resistance curve for a bottom trawl as compared to that predicted on the basis of the theory presented earlier.

In order to establish the effect of the bottom on the error of the estimate, the total resistance for a midwater trawl was calculated. The doors of a midwater trawl never touch the bottom and the only resistance acting on them is hydrodynamic. The effect of the ocean bottom on the pressure distribution along the lower portion of the net is also absent when trawling in midwater. These factors, in addition to the fact that the footrope no longer touches the bottom, should reduce the degree of error when a midwater trawl is considered. The results of the computation for the specific case of the Christensen midwater trawl are given in figure 21 along with field measurements reported Taber, (1969). The agreement between theory and experiments in that case is closer. Furthermore, it seems reasonable to say that component interaction does not affect the overall trawl resistance significantly, and the bottom effects are the largest source of error in the estimate.

The method of computing the resistance of trawling gear presented should be used with caution and it appears to apply

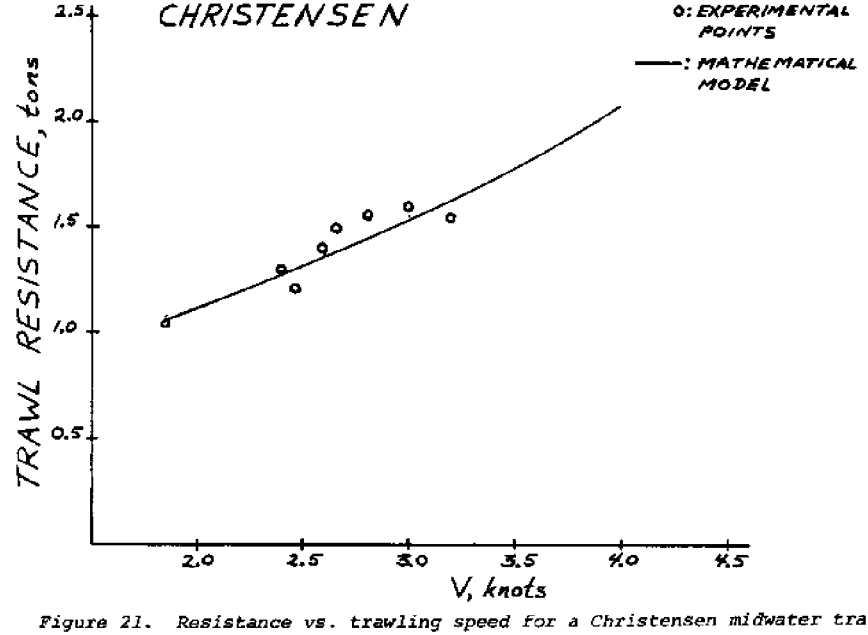

Figure 21. Resistance vs. trawling speed for a Christensen midwater trawl.

better to the case of midwater trawls where the effects of the ocean bottom are not present.

Relationship between Forces and Trawl Geometry

Assume the trawl has the simplified shape shown in figure 22 as it moves at a speed V parallel to y. ABC is the headline and ADC is the footrope. The upward lifting force, L, exerted by the floats on the headline is assumed to be concentrated at point B. Likewise, the downward sinking force acting on the footrope is taken to be concentrated at point D. For ease of calculations it is assumed that the sinking force has also a value of L equal to the lifting force. The spreading force of each door, N, is assumed to act at points A and C. The net bag resistance, D_T, acts parallel to the y axis. The force, N, acts parallel to the x axis and the force, L, acts parallel to the z axis. Let AB = BC = CD = DA and AE = BE = CE = DE = h. Also let AC = 2b and BD = 2a.

Assuming that the "trawl" of figure 22 is made up of four triangular panels, one can obtain from equilibrium conditions

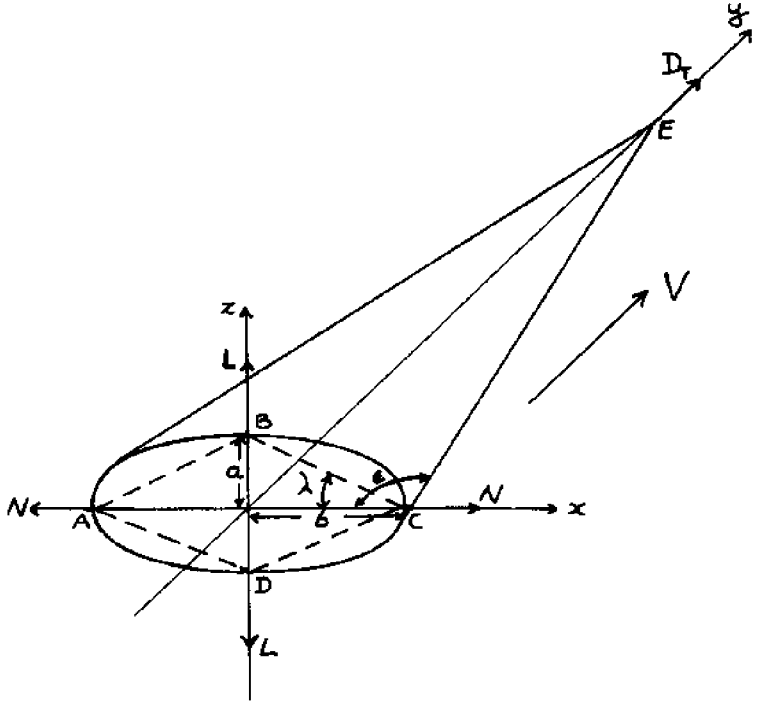

Figure 22. Simplified mouth configuration for a typical trawl.

the tension forces set up along the edges of these panels by the joint action of D_T, N, and L. The tension that opposes the resistance force D_T is taken entirely along EC and EA for ease of analysis. However, it could be split in four ways along EA and EB, EC and ED. Thus, from figure 23, the condition for equilibrium at point E is

$$D_T = 2\omega \sin\epsilon$$

where ω is the tension along EA and EC.

The tension δ along the perimeter of the mouth ABCD is shown in figure 24 along with the component of the tension ω. The condition for equilibrium at point B is

$$L = 2\delta \sin\lambda$$

The condition for equilibrium at point C is

$$N = 2\delta \cos\lambda + \omega\cos\epsilon$$

Substituting

$$N = L\,\mathrm{ctg}\lambda + \frac{D_T}{2}\,\mathrm{ctg}\epsilon \qquad (7)$$

Equation 7 relates the forces N, L and D_T with the geometric configuration of the trawl represented by the angles ϵ and λ. Furthermore, N and D_T are functions of trawling speed V so that equation 7 describes the effect of speed on the configuration of the net bag also.

The next step is to represent the angles in terms of trawl dimensions. From geometric considerations

$$\mathrm{ctg}\lambda = \frac{b}{a} \quad \text{and} \quad \mathrm{ctg}\epsilon = \frac{b}{(h^2-b^2)^{1/2}}$$

Substituting into equation 7

$$N = L\,\frac{b}{a} + \frac{D_T}{2}\,\frac{b}{(h^2-b^2)^{1/2}} \qquad (8)$$

Thus an equation relating N, L, D_T, a, b, and h has been obtained. and $D_T/2$ is half the drag of the net bag with all of its lines, floats and cod end.

$$D_T = D_{\text{cone}} + D_{\text{cod end}} + D_{\text{lines}} + D_{\text{Ground Warps}} + D_{\text{floats}}$$

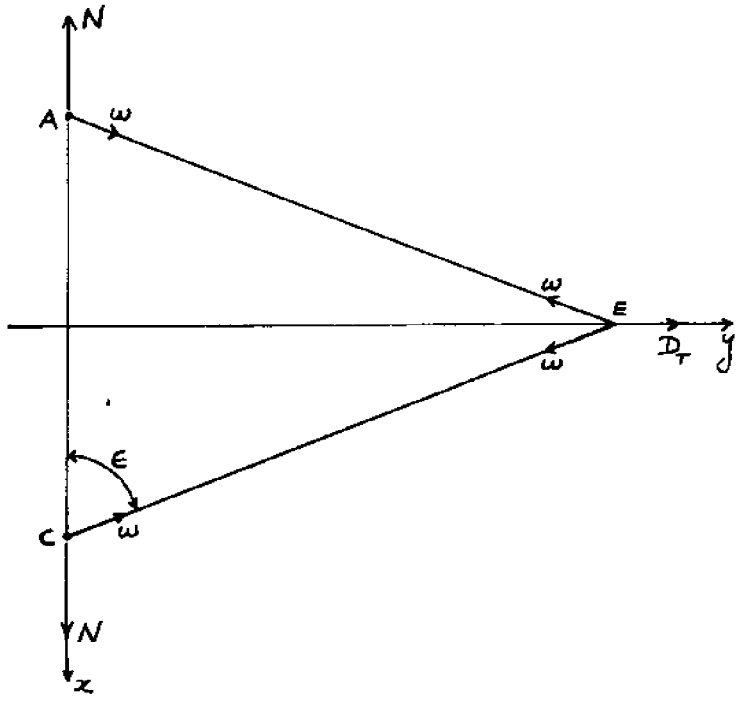

Figure 23. Top view of the simplified trawl.

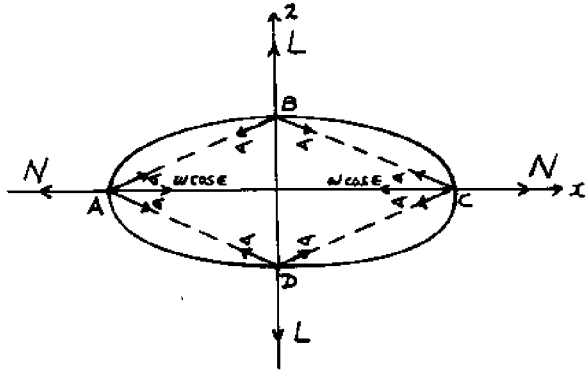

Figure 24. Front view of the simplified trawl.

The conical portion of the net bag contributed a drag force which was proportional to the cross-sectional area of the mouth, πab, according to equation 5. The force L is essentially the buoyant force contributed by the floats. If there are n_f spherical floats of radius r_{fl} then

$$L = n_{fl} \left[\frac{4}{3} \pi r^3_{fl} (\rho g)_{sw} - W_{fl}\right]$$

where $(\rho g)_{sw}$ is the specific gravity of salt water with a value of 64 $\frac{lbf}{ft^3}$ and W_{fl} is the weight of each float. Finally, the

spreading force, N, of the doors is given by

$$N = C_L \frac{1}{2} \rho V^2 A_D$$

for a midwater trawl, where C_L is the lift coefficient, ρ is the density of seawater, V is the trawling speed and A_D is the area of the door. For a bottom trawl, N has an additional component due to the sideways ground reaction N_{Gx} and in that case

$$N = C_L \frac{1}{2} \rho V^2 A_D + N_{Gx}$$

Substituting into equation 8 a general relationship describing the configuration adopted by a trawl as it moves through the water is obtained. This relationship requires a numerical solution since a and b are unknown.

If instead of using the two dimensions a and b one uses the angles ϵ and λ and writes equation 7 in terms of functions of velocity, then

$$N (V^2) = L \operatorname{ctg} \lambda + D_T (V^2) \operatorname{ctg} \epsilon \qquad (9)$$

Equation 9 indicates that changing the speed from zero to infinity decreases the angle λ from $\frac{\pi}{2}$ to zero. When λ is $\frac{\pi}{2}$ the vertical opening 2a is a maximum and the horizontal opening 2b is a minimum. When λ is zero the vertical opening 2a is a minimum and the horizontal opening 2b is a maximum. These effects are better understood by looking at figure 22. A more realistic range of speeds found in commercial trawling will lie between these two extremes. However, the behavior indicated by equation 9 will be similar.

Defining an "infinitely long" trawl as one for which $\frac{h}{2b} \geq 4$ or $\frac{h}{b} \geq 8$, then the above derived equations can be simplified in order to obtain approximate values of a and b.

Equation 8 can be written:

$$N = L \left(\frac{b}{a}\right) + \frac{D_T}{2} \frac{1}{\left[\left(\frac{h}{b}\right)^2 - 1\right]^{1/2}}$$

For an infinitely long trawl let $\frac{h}{b} = 8$

$$N = L \left(\frac{b}{a}\right) + 0.063\ D_T \qquad (10)$$

Since D_T is a function of a, b, and h, the above equation can be used to determine either the force N which the doors have to provide for a desired mouth opening or the ratio b/a when N is known. Knowledge of the approximate value of b/a as a function of speed is an important consideration when the objective is to trawl at the speed which gives the most ideal trawl mouth configuration for existing conditions.

Equation 10 implies previous knowledge of the hydrodynamic lift characteristics of the doors as well as of the nature of the ground reaction forces. Some work has been done in these two areas but further experimentation is required for various door geometries and types of ocean bottoms.

CONCLUSIONS

An analysis of the drag of a fishing trawl was accomplished by considering the drag of each of its components. Formulas were developed for calculation of the resistance of each component of the trawl based on the hydrodynamic drag coefficients available from other sources. The formula giving the drag of the net bag was based on the drag of an equivalent cone with an elliptical cross-section. The area of the net was represented by a solidity ratio which accounts for the permeability of the trawl netting. It was shown that the drag of the net bag is based on the area of the mouth, the length of the net and the solidity of the net.

The total drag was computed as the sum of the component drags; this gives valuable insight into the relative importance of the different parts of the trawl from the point of view of drag. Table 2 gives the percentage drag contribution of the different parts of the fishing trawl for a Yankee 35 bottom trawl and a Christensen midwater trawl. It can be seen from the table that the doors and the net bag are the biggest contributors to the drag of the trawl, accounting for over two-thirds of the total. The cod end becomes important only when filled, at which time the fishing operation stops. Hence, its drag is of lesser importance.

TABLE 2. Drag contribution by the components of a fishing trawl.

	Percent of Total Drag	
Component	Yankee 35 Bottom Trawl (at 3 Knots)	Christensen Midwater Trawl (at 4 Knots)
Cod End(filled)	18.0	20.0
Small Lines	3.3	3.0
Net Bag	27.7	38.0
Floats	3.0	3.0
Doors	44.0	34.0
Towing Warps	4.0	2.0

APPENDIX Equilibrium Equations for the Towing Warps Using Pode's Analysis

Figure A.1 shows the coordinate system used in writing the equilibrium equations for a towed cable.

$$dT = -P(\phi)\, ds$$

$$T d\phi = -Q(\phi)\, ds$$

Dividing

$$\frac{dT}{T} = \frac{P(\phi)\, d\phi}{Q(\phi)}$$

Let P_o be any point on the cable. Integrating along the cable from P_o to any point P where the tension is T and angle is ϕ,

$$\frac{T}{T_o} = e^{\int_{\phi_o}^{\phi} \frac{P(\phi)\, d\phi}{Q(\phi)}}$$

Combining

$$ds = \frac{T_o}{-Q(\phi)}\, e^{\int_{\phi_o}^{\phi} \frac{P(\phi)}{Q(\phi)}\, d\phi}\, d\phi$$

and

$$s = \int_{\phi_o}^{\phi} \frac{T_o}{-Q(\phi)}\, e^{\int_{\phi_o}^{\phi} \frac{P(\phi)}{Q(\phi)}\, d\phi}\, d\phi$$

now

$$dx = (\cos\phi)\, ds, \qquad dy = (\sin\phi)\, ds$$

it follows

$$x = \int_{\phi_o}^{\phi} \frac{T_o}{-Q(\phi)}\, e^{\int_{\phi_o}^{\phi} \frac{P(\phi)}{Q(\phi)}\, d\phi}\, \cos\phi\, d\phi$$

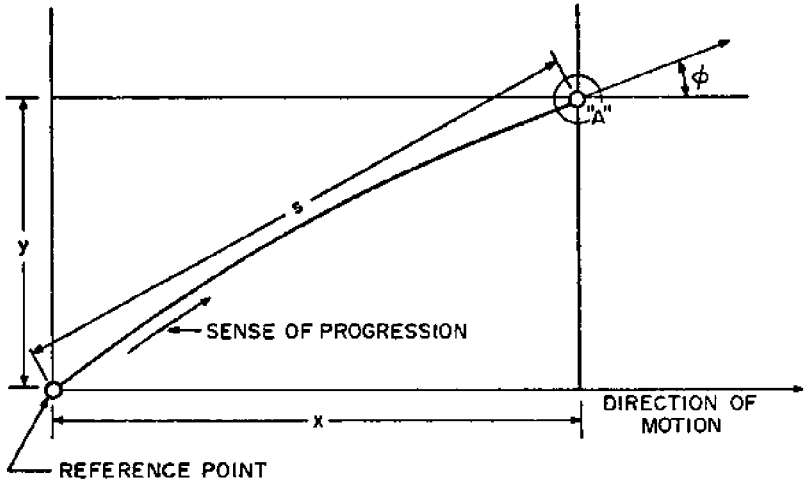

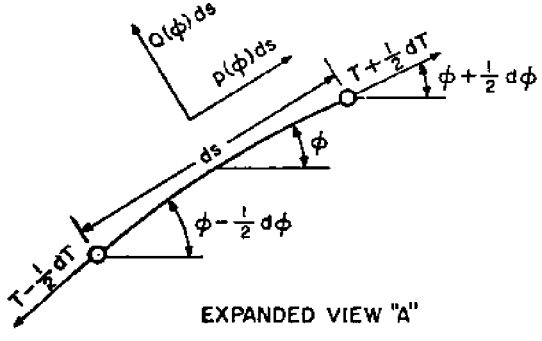

Figure A.1. Coordinate system for a towing cable.

and

$$y = \int_{\phi_o}^{\phi} \frac{T_o}{-Q(\phi)} \, e^{\int_{\phi_o}^{\phi} \frac{P(\phi)}{Q(\phi)} \, d\phi} \sin\phi \, d\phi$$

It is convenient to express T, s, x, and y nondimensionally. T is already in nondimensional form. A unit length is desired in order to put s, x, and y in nondimensional form. Choosing the length of cable, which when perpendicular to the flow has a drag equal to the tension, T_o. If R is the drag per unit length of cable when the cable is perpendicular to the flow, the following nondimensional values are obtained.

$$p = \frac{P(\phi)}{R}$$

$$q = \frac{Q(\phi)}{R}$$

$$\tau = \frac{T}{T_o} = e^{\int_{\phi_o}^{\phi} \frac{p}{q}\, d\phi}$$

$$\sigma = \frac{Rs}{T_o} = \int_{\phi_o}^{\phi} \frac{-\tau}{q}\, d\phi$$

$$\xi = \frac{Rd}{T_o} = \int_{\phi_o}^{\phi} \frac{\tau\cos\phi}{-q}\, d\phi$$

$$\eta = \frac{R_Y}{T_o} = \int_{\phi_o}^{\phi} \frac{\tau\sin\phi}{-q}\, d\phi$$

The cable functions P (ϕ) and Q(ϕ) can also be written in terms of the drag R, when the cable is perpendicular to the flow; the tangential component of the hydrodynamic force, F; and the weight of the cable in water W. The forces R, F, and W are all per unit length of cable. Thus, according to figure A.2,

$$P(\phi) = \frac{-F\cos\phi}{|\cos\phi|} - W\sin\phi$$

$$Q(\phi) = R\,\sin\phi/|\sin\phi| - W\cos\phi$$

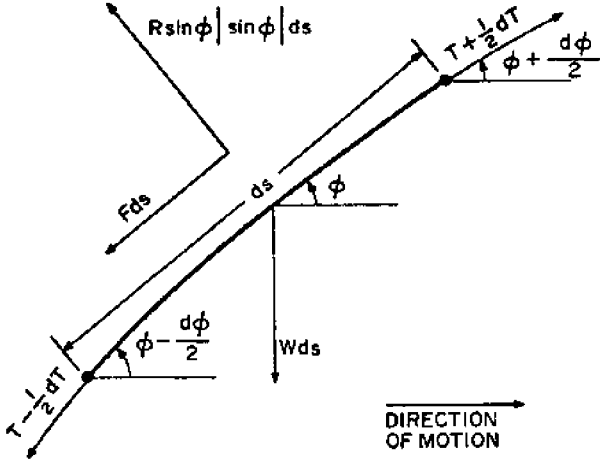

Figure A.2. Forces acting on a cable element.

Letting the angle at which $Q(\phi)$ becomes zero be called the critical angle ϕ_c and assuming ϕ_c lies in the range $0 \leq \phi_c \leq \pi$

$$R \sin^2\phi_c - W\cos\phi_c = 0; \quad \cos^2\phi_c + \frac{W}{R}\cos\phi_c - 1 = 0$$

This equation has two roots. When the cable is negatively buoyant, W is positive and

$$\cos\phi_c = \frac{-W}{2R} + \sqrt{\left(\frac{W}{2R}\right)^2 + 1}$$

When the cable is positively buoyant, W is negative and

$$\cos\phi_c = \frac{-W}{2R} - \sqrt{\left(\frac{W}{2R}\right)^2 + 1}$$

The case of the towing warp of a trawl corresponds to the case of a negatively buoyant cable. Consequently W is positive and ϕ_c ranges from zero when $W/R = 0$ to $\pi/2$ when W/R is infinite. Now W is constant for a given cable but the force R is a function of speed. This makes the cable functions dependent on speed and these become

$$\ln\tau = \int_{\phi_o}^{\phi} \frac{\frac{\cos\phi}{|\cos\phi|} + w\sin\phi}{-\sin\phi/|\sin\phi| + w\cos\phi}\, d\phi; \qquad \sigma = \int_{\phi_o}^{\phi} \frac{\tau}{-\sin\phi/|\sin\phi| + w\cos\phi}\, d\phi$$

$$\xi = \int_{\phi_o}^{\phi} \frac{\tau\cos\phi}{-\sin\phi/|\sin\phi| + w\cos\phi}\, d\phi; \qquad \eta = \int_{\phi_o}^{\phi} \frac{\tau\sin\phi}{-\sin\phi/|\sin\phi| + w\cos\phi}\, d\phi$$

where $f = F/R$ and $w = W/R$. Pode (1951) calculated the cable functions by dividing the integrations into the three quadrants in which the angle ϕ may fall as shown in figure A.3. The case of the towing warp corresponds to quadrant 3 where $\pi \leq \phi \leq \pi + \phi_c$. If the reference point is taken where $\phi = \pi$ i.e. where the cable is parallel to the flow, the cable functions for quadrant 3 are given by

$$\ln\tau = \int_{\pi}^{\phi} \frac{-f + w\sin\phi}{\sin^2\phi + w\cos\phi}\, d\phi$$

$$\sigma = \int_{\pi}^{\phi} \frac{\tau}{\sin^2\phi + w\cos\phi}\, d\phi$$

$$\xi = \int_{\pi}^{\phi} \frac{\tau\cos\phi}{\sin^2\phi + w\cos\phi}\, d\phi$$

$$\eta = \int_{\pi}^{\phi} \frac{\tau\sin\phi}{\sin^2\phi + w\cos\phi}\, d\phi$$

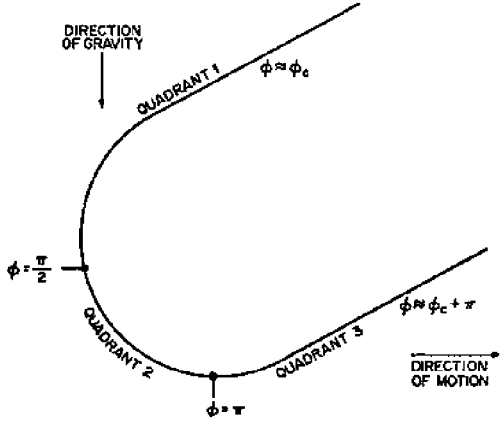

Figure A.3. Cable quadrants.

Numerical Example Using Pode's Analysis

Figure A.4 shows a trawl as it is towed over the ocean bottom by a trawler using negatively buoyant cables. The drag of the towing warps at a given trawling speed, D_w, is given by

$$1/2\ D_w = T_{2x} - T_{1x}$$

where

$$T_{2x} = T_2 \cos\theta_2$$

and

$$T_{1x} = T_1 \cos\theta_1$$

The warp tension at the door, T_1, is given by

$$T_1 = \sqrt{(1/2\ D_T + R_D)^2 + T_y^2}$$

T_1 can be obtained from the output of the computer program for the trawling gear resistance, and at 3 knots T_1 is 1600.63 lbf. The program output also gives the warp angle at the door, θ_1; the warp drag per unit length of cable, R; and the towing warp critical angle, ϕ_c. At a speed of 3 knots these values are:

$$\theta_1 = 2.2^o$$

$$R = 1.56 \text{ lbf/ft}$$

$$\phi_c = 32^o$$

The ratio f can be taken as 0.02 for common cables such as the warps.

$$\nu_2 = \frac{Ry}{T_1}$$

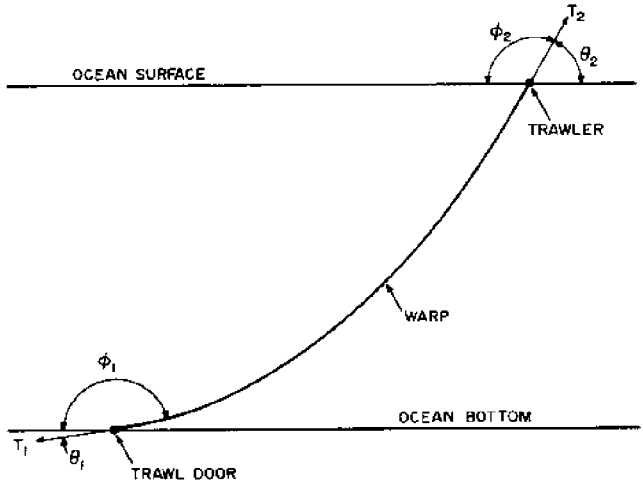

Figure A.4. Towing warp configuration during trawling.

If the depth of trawling, y, is about 150 ft. then η_{2^o} = -.13937. From Pode's tables interpolating for $\phi_c = 32^o$, the magnitude of τ_2 and $180 - \phi_2$ are obtained

$$\tau_2 = 1.0616$$

$$180 - \phi_2 = 17^o$$

The angle θ_2 is defined in figure A.4 and it follows that θ_2 is 17^o.

The function τ_2 is defined as T_2/T_1 so that

$$T_2 = \tau_2 T_1$$

$$= 1.0616 \times 1600.63$$

$$= 1699.23 \text{ lbf.}$$

$$T_{1x} = 1600.63 \cos 2.2^o$$

$$= 1599.35 \text{ lbf.}$$

$$T_{2x} = 1699.23 \cos 17^o$$

$$= 1624.97 \text{ lbf.}$$

Thus

$$D_w = 2(1624.97 - 1599.35)$$

$$= 51.3 \text{ lbf.}$$

References

1. Carrothers, P.J.G., Foulkes, T.J., Connors, M.P., Walker, A.G. (1969) Data on the Engineering Performance of Canadian East Coast Groundfish Otter Trawls, Fisheries Research Board of Canada Technical Report No. 125.

2. Crewe, P.R. (June, 1964) "Some of the General Engineering Principles of Trawl Gear Design," Modern Fishing Gear of the World.

3. Hoerner, S.F. (1965) Fluid Dynamic Drag.

4. Kowalski, T., Giannotti, J. (1974) Calculation of Fishing Net Drag, Marine Technical Report Series No. 15, University of Rhode Island.

5. Pode, L. (1951) Tables for Computing the Equilibrium Configuration of a Flexible Cable in a Uniform Stream, DTMB Report 687, NS 830-100.

6. Taber, R.E. (1969) The Dynamics of European Wing Trawls, Marine Leaflet Series No. 3, University of Rhode Island.